


Article

N6-Methyladenosine Regulates the Expression and Secretion of TGF β 1 to Affect the Epithelial–Mesenchymal Transition of Cancer Cells

Jiexin Li ¹, Feng Chen ¹, Yanxi Peng ¹, Ziyang Lv ¹, Xinyao Lin ¹, Zhuojia Chen ^{2,*} and Hongsheng Wang ^{1,*} 

¹ Department of Microbial and Biochemical Pharmacy, School of Pharmaceutical Sciences, Sun Yat-sen University, Guangzhou 510006, China; lijixin3@mail.sysu.edu.cn (J.L.); chen57@mail2.sysu.edu.cn (F.C.); yx117pengyanxi@163.com (Y.P.); lvzy5@mail2.sysu.edu.cn (Z.L.); linxy49@mail2.sysu.edu.cn (X.L.)

² Sun Yat-sen University Cancer Center, State Key Laboratory of Oncology in South China, Collaborative Innovation Center for Cancer Medicine, Guangzhou 510060, China

* Correspondence: chenzhj@sysucc.org.cn (Z.C.); whongsh@mail.sysu.edu.cn (H.W.); Tel.: +86-020-87343759 (Z.C.); +86-020-39943024 (H.W.)

Received: 16 December 2019; Accepted: 19 January 2020; Published: 25 January 2020



Abstract: N6-methyladenosine (m⁶A) is the most abundant modification on eukaryotic mRNA, which regulates all steps of the mRNA life cycle. An increasing number of studies have shown that m⁶A methylation plays essential roles in tumor development. However, the relationship between m⁶A and the progression of cancers remains to be explored. Here, we reported that transforming growth factor- β (TGF β 1)-induced epithelial–mesenchymal transition (EMT) was inhibited in methyltransferase-like 3 (METTL3) knockdown (Mettl3^{Mut/-}) cells. The expression of TGF β 1 was up-regulated, while self-stimulated expression of TGF β 1 was suppressed in Mettl3^{Mut/-} cells. We further revealed that m⁶A promoted TGF β 1 mRNA decay, but impaired TGF β 1 translation progress. Besides this, the autocrine of TGF β 1 was disrupted in Mettl3^{Mut/-} cells via interrupting TGF β 1 dimer formation. Lastly, we found that Snail, which was down-regulated in Mettl3^{Mut/-} cells, was a key factor responding to TGF β 1-induced EMT. Together, our research demonstrated that m⁶A performed multi-functional roles in TGF β 1 expression and EMT modulation, suggesting the critical roles of m⁶A in cancer progression regulation.

Keywords: m⁶A; TGF β 1; EMT

1. Introduction

In eukaryotes, gene expression is regulated by transcriptional and post-transcriptional processes. Among the over 100 modifications in mRNA, N6-methyladenosine (m⁶A) is one of the most abundant internal modifications [1–3]. This methylation process is catalyzed by “writer” methyltransferases, including methyltransferase-like 3 and 14 (METTL3 and METTL14) and other cofactors, such as Wilm’ tumor-1-associated protein (WTAP). m⁶A-modified mRNA is recognized by distinct “reader” proteins containing the YT521-B homology (YTH) domain, such as cytoplasmic proteins YTHDF1, YTHDF2, YTHDF3, and nuclear proteins YTHDC1 and YTHDC2. “Eraser” demethylases, alkylation repair homolog protein 5 (ALKBH5), and the fat mass and obesity-associated protein (FTO) are responsible for maintaining the balance of m⁶A methylation and demethylation in mammalian cells [4,5].

A growing body of work provides evidence showing that m⁶A mRNA modification acts as a regulator of the mRNA life cycle, including pre-mRNA splicing [6–8], nucleo-cytoplasmic export [5,9,10], mRNA decay [11,12], and mRNA translation [13,14]. The METTL3–METTL14 heterodimeric complex generates m⁶A on mRNA, where METTL3 contributes the catalytic residues and METTL14 provides

structural supports for METTL3 [15–17]. Acting as the executor of m⁶A modification, METTL3 plays crucial roles in various biological processes, including tumor development [18,19]. For instance, METTL3 is necessary for the development and maintenance of mouse and human myeloid leukemia [20]. Our recent study indicated that METTL3 regulated the epithelial–mesenchymal transition (EMT) of cancer cells via Snail translation [21]. Although associations between m⁶A methylation and tumorigenesis, especially EMT process, have arisen for the last decade, the detailed mechanisms remained to be elucidated.

EMT of cancer can be induced by a plethora of signaling pathways, and transforming growth factor β (TGF β) is the prominent EMT inducer in cancer cells [22]. TGF β , which contains three isoforms, TGF β 1, TGF β 2, and TGF β 3, is synthesized as a pro-protein monomer. During the maturation, the TGF β dimer forms a complex with latent TGF β binding proteins (LTBPs), called a latent complex [23,24], which is crucial for the secretion of TGF β and the activation of TGF β receptor (TGFR)-mediated cell signaling [25,26]. TGF β induces the expression of many other growth factors and cytokines to initiate EMT, while also cooperating with the initial stimulus of TGF β to stimulate self-expression, which is necessary for sustained signaling, which continually supports the long process of EMT [22,27].

In this study, we investigate the potential effects of m⁶A on the TGF β 1-induced EMT of cancer cells. Our data reveal that TGF β 1-induced EMT is suppressed in METTL3 knockdown cells (Mettl3^{Mut/-}). However, the expression of TGF β 1 is enhanced in Mettl3^{Mut/-} cells but decreased in TGF β 1-treated Mettl3^{Mut/-} cells. We demonstrate that m⁶A regulates the stability and translation of TGFB1 mRNA. In addition, METTL3 modulates the secretion and activation of TGF β 1. Besides this, we further reveal that the suppression of TGF β 1-induced EMT in Mettl3^{Mut/-} cells is mainly due to the downregulation of Snail. Together, our data suggest that m⁶A performs multi-functional roles in the TGF β 1 expression and EMT modulation of cancer cells.

2. Materials and Methods

2.1. Ethics Statement

All animal experiments were conducted according to the guidelines of the Animal Care and Use Committee of Sun Yat-sen University. Animals were maintained in accordance to the guidelines of the American Association of Laboratory Animal Care.

2.2. Cell Culture, Treatments, and Transfection

Mettl3^{Mut/-} cells were generated as previously described using the CRISPR-Cas9 editing system [28]. Both HeLa cells and Mettl3^{Mut/-} cells were cultured in Dulbecco's Modified Eagle Medium (DMEM, GIBCO, Carlsbad, CA, USA) supplemented with 10% fetal bovine serum (FBS) at 37 °C in a 5% CO₂ atmosphere. For TGF β 1 treatments, 10 ng/mL TGF β 1 (PeproTech, Rocky Hill, NJ, USA) was added into cell culture medium for the indicated time points. For transfection, plasmids were transfected into cells using Lipofectamine 3000 reagent (Invitrogen Life Technology, Carlsbad, CA, USA), following the manufacturer's instructions.

2.3. Plasmid Constructions

The 5'UTR region of TGFB1 was cloned into the pGL3–basic vector in the front of the F-Luc gene (pGL3–basic–WT–5'UTR). The CDS region of TGFB1 was cloned into the pcDNA3–HisMax vector (pcDNA3–WT–CDS). Mutagenesis of m⁶A motifs (GGAC to GGCC) in both pGL3–basic–WT–5'UTR and pcDNA3–WT–CDS was performed using a site-directed mutagenesis kit (Thermo Fisher Scientific, Waltham, MA, US). Primers for mutagenesis are listed in Additional file 1: Table S1. The CDS region of the TGF β binding protein (LTBP1) was cloned into the pHM6 vector.

2.4. Wound Healing Assay

Cells were seeded and cultured until 90% confluent monolayer. Cells were then scratched by a sterile pipette tip and applied for treatments in FBS-free medium, as indicated in the text. The migration distances of cells into the scratched area were measured in 10 randomly chosen fields under microscope.

2.5. In Vitro Invasion Assay

The transwell assay was conducted by CytoSelect™ 24-well Cell Invasion assay kits. Briefly, polycarbonate filters (8 µm pore size, Corning) coated with 50% Matrigel (BD bioscience, Bedford, MA) were used to separate the upper and lower chambers. Then, 5×10^4 cells in 200 µL culture medium supplemented with 0.1% FBS were added into the upper chamber, while 600 µL medium supplemented with 10% FBS was added into the lower chamber and served as a chemotactic agent. For TGFβ1 treatments, 10 ng/mL TGFβ1 was supplemented in culture medium. After 48 h incubation, the invaded cells onto the lower chamber were fixed, stained, and counted under the upright microscope (five fields per chamber).

2.6. Western Blot Analysis

Total cell lysates were collected as previously described [29]. The primary antibodies used for immunoblotting included anti-TGFβ1 (21898-1-AP, Proteintech, Wuhan, China), anti-E-cad (ab1416, Abcam, Cambridge, MA, USA), anti-FN (sc-52331, Santa Cruz Biotechnology, Santa Cruz, CA, USA), anti-Snail (ab53519, Abcam), anti-METTL3 (ab195352, Abcam), anti-LTBP1 (A15287, Abclonal), anti-LTBP2 (PA5-51930, Invitrogen), anti-LTBP3 (A15687, Abclonal, Wuhan, China), anti-SMAD2 (ab40855, Abcam), anti-pSMAD2 (3108, Cell signaling technology, Danvers, MA, USA). The immunoblotting results presented were representatives from at least three independent experiments.

2.7. RNA Extraction and Quantitative Real-Time PCR (qRT-PCR)

RNA extraction with Trizol (Invitrogen) and real time PCR were performed according to the protocol used in our previous study [21]. The primers of targeted genes were as follow: TGFβ1, forward 5'-CGCGTGCTAATGGTGGAAA-3' and reverse 5'-CGCTTCTCGGAGCTCTGATG-3'; pre-TGFβ1 forward 5'-CGTGCTAATGGTGGAAACCCA-3' and reverse 5'-CAGTGCCATCCTCTTTTCGGA-3'; HPRT, forward 5'-TGACACTGGCAAACAATGCA-3' and reverse 5'-GGTCCTTTTACCAGCAAGCT-3'; GAPDH, forward 5'-GTCTCCTCTGACTTCAACAGC G-3' and reverse 5'-ACCACCCTGTTGCTGTAGCCAA-3'; CDH1, forward 5'- GCCTCCTGAAAAGAGAGTGGAAAG-3' and reverse 5'-TGGCAGTGTCTCTCCAAATCC G-3'; 18S, forward 5'- CGGACAGGATTGACAGATTGATAGC-3' and reverse 5'- TGCCAGAGTCTCGTTCGTTATCG-3'; MALAT1, forward 5'-GCTTGGCTTCTTCTGGACTCA-3' and reverse 5'- TCGCGAGCTTCACCATGA-3'; 7SL, forward 5'- GCACTAAGTTCGGCATCAATATG-3' and reverse 5'-AGTGCAGTGGCTATTACAG-3'; VIM, forward 5'-AGGCAAAGCAGGAGTCCACTGA-3' and reverse 5'-ATCTGGCGTTCCAGGGACTCAT-3'; SNAI1, forward 5'-TGCCCTCAAGATGCACATCCGA-3' and reverse 5'- GGGACAGGAGAAGGGCTTCTC-3'; METTL3, forward 5'-CTATCTCCTGGCACTCGCAAGA-3' and reverse 5'-GCTTGAACCGTGCAACCACATC-3'; LTBP1, forward 5'-GCCCTAATGGTGTGAGTGTGTTGA-3' and reverse 5'-AGATCACAGGGGGATCAGG-3'; LTBP2, forward 5'-TGCCCTAGTGGAAAAGGCTA-3' and reverse 5'-TCACACACTCATCCGCATCT-3'; LTBP3, forward 5'-CACCTGAGGACACAGAGGAAG-3' and reverse 5'-GAGATCAGCTCGGGGTAGG-3'; FLUC, forward 5'- GGCCTGACAGAAACAACCAG -3' and reverse 5'- AAGTCCACCACCTTAGCCTC -3'; RLUC, forward 5'-CGCTATTGTCGAGGGAGCTA -3' and reverse 5'- GCTCCACGAAGCTCTTGATG -3'; METTL3 (mouse), forward 5'- CAGTGCTACAGGATGACGGCTT-3' and

reverse 5'- CCGTCCTAATGATGCGCTGCAG-3'; GAPDH (mouse), forward 5'- CATCACTGCCACCCAGAAGACTG-3' and reverse 5'- ATGCCAGTGAGCTTCCCGTTCAG-3'; TGFB1 (mouse), forward 5'- TGATACGCCTGAGTGGCTGTCT-3' and reverse 5'- CACAAGAGCAGTGAGCGCTGAA-3'. GAPDH was used as a control for normalization.

2.8. m⁶A RNA-Immunoprecipitation (RIP) qPCR

The m⁶A-qRT-PCR was conducted according to previous studies, with slight modifications [30]. Briefly, total RNAs (200 ug) extracted by Trizol were used for immunoprecipitation by the m⁶A antibody (Synaptic Systems) or IgG in IP buffer (150 mM NaCl, 0.1% NP-40, 10 mM Tris, pH 7.4, 100U RNase inhibitor) to obtain the m⁶A pull down portion. The m⁶A RNAs were immunoprecipitated by Dynabeads[®] Protein A (ThermoFisher Scientific) and eluted twice by elution buffer (5 mM Tris-HCL pH 7.5, 1 mM EDTA pH 8.0, 0.05% SDS, 20 mg/mL Proteinase K). m⁶A-IP RNAs were precipitated by ethanol and the RNA concentration was measured with a Qubit[®] RNA HS Assay Kit (ThermoFisher Scientific). A total of 2 ng of total RNA (Input) and m⁶A-IP RNA were used as the template for qRT-PCR. HPRT1 acted as the internal control of the input samples, since it did not contain m⁶A peaks from the m⁶A profiling data [12]. The student's *t*-test was used for statistical analysis.

2.9. Cell Fractionation Assay

A total of 10⁷ cells were rinsed with PBS once and then pelleted. Fractionation of the nuclear and cytoplasmic samples was performed using an NE-PER(R) nuclear and cytoplasmic extraction kit (Thermo Fisher). Total RNA in the nuclear and cytoplasmic fractions was extracted by Trizol. The nuclei–cytoplasm ratio was determined by the mRNA levels of targets in the nuclear and cytoplasmic fractions, which were normalized to the levels of nuclear MALAT1 RNA and cytoplasmic 7SL RNA, respectively [31].

2.10. mRNA Stability Assay

HeLa or Mettl3^{Mut/-} cells were seeded on six-well plate one day before treatment. A total of 5 µg/mL actinomycin D (Act-D) was added in serum-free culture medium for the indicated times. Cells were washed by PBS and subjected to isolate total RNA by Trizol. RNA concentrations were quantified by a Qubit[®] RNA HS Assay Kit (ThermoFisher Scientific) and qRT-PCR performed, where 18S mRNA acted as the internal control.

2.11. Polysome Profiling

Polysome profiling was conducted according to previous studies [11]. Two 10 cm dishes of HeLa or Mettl3^{Mut/-} cells were incubated with 100 µg/mL cycloheximide (CHX) for 5 min at 37 °C before collection. The culture medium was removed and cells were washed with cold PBS with 100 µg/mL CHX. A total of 300 µL lysis buffer per dish (10 mM Tris, pH 7.4, 150 mM KCl, 5 mM MgCl₂, 100 µg/mL CHX, 0.5% Triton X-100, freshly added protease inhibitor, and RNase inhibitor) was added to cells and kept on ice for 15 min with pipetting. Cell suspension was centrifuged at 13,000g for 15 min, and supernatant was collected and tested at 260 nm. A 5/50% *w/v* sucrose gradient was prepared in lysis buffer without Triton X-100. Clear cell lysate was loaded on the sucrose gradient and centrifuged at 4 °C for 4 h at 27,500 rpm. The sample was then fractionated and analyzed by Gradient Station (BioCamp, New Brunswick, Canada). Fractionated samples were then used to isolate total RNA for qRT-PCR.

2.12. Dual-Luciferase Reporter Assay

The luciferase assay was performed using reporter lysis buffer (Promega, Milan, Italy) and luciferase assay reagents according to the manufacturer's instructions. Briefly, cells were co-transfected with pGL3–basic–WT–5'UTR or pGL3–basic–Mut–5'UTR and TK-Rluc reporter in six-well plate for 24 h.

Cells were then analyzed with the Dual-Glo Luciferase Assay system (Promega). Renilla Luciferase (R-Luc) was used to normalize firefly luciferase (F-Luc) activity.

2.13. TGF β 1 Secretion Detection

Cell culture medium was collected after 48 h incubation with TGF β 1. TGF β 1 secretion was detected by a TGF β 1 ELISA kit, following the manufacturer's instruction (Quantikine ELISA Kits, R & D systems, Minneapolis, MN, USA). The results were calculated by reference to the standard curve provided by the manufacturer standards, within the range from 0 pg/mL to 2000 pg/mL. Secreted TGF β 1 levels from cells with or without treatment were normalized to plain culture medium or TGF β 1-treated culture medium, respectively.

3. Results

3.1. METTL3 Is Essential for TGF β 1-Induced EMT

To verify the effect of METTL3 in HeLa cells, we constructed METTL3 knockdown HeLa cells (Mettl3^{Mut/-}) by CRISPR/Cas9 system for studies. The enzymatic activities of METTL3 were detected by LC-MS/MS (Additional file 1: Figure S1a) [28]. Results showed that both the cell migration and cell invasion abilities of Mettl3^{Mut/-} cells decreased significantly compared to control cells (Figure 1a,b). Consistently, the down-regulation of fibronectin (FN) and up-regulation of E-cadherin (E-cad) were observed in Mettl3^{Mut/-} cells (Figure 1c), indicating that METTL3 modulated both cell migration and invasion in HeLa cells.

To further investigate the effect of METTL3 on EMT, we treated cells with 10 ng/mL TGF β 1, which has been considered to be the major EMT inducer in cancer cells. Both wound healing assay and Transwell assay showed that cell migration and invasion of control HeLa cells were successfully enhanced by TGF β 1, while there was no significant difference in Mettl3^{Mut/-} cells (Figure 1a,b). Western blot analysis showed up-regulation of FN and down-regulation of E-cad in TGF β 1-treated HeLa cells; however, neither FN or E-cad in TGF β 1-treated Mettl3^{Mut/-} cells showed significant change (Figure 1c), suggesting that the EMT process in Mettl3^{Mut/-} cells was inhibited even in the presence of TGF β 1. We further re-introduced METTL3 into Mettl3^{Mut/-} cells, TGF β 1-treated Mettl3^{Mut/-} cells regained both cell migration and invasion abilities (Additional file 1: Figure S1b,c). Nevertheless, up-regulation of FN and down-regulation of E-cad were observed in Mettl3^{Mut/-} cells overexpressing METTL3, and TGF β 1 treatments further enhanced these trends (Additional file 1: Figure S1d). Together, our data suggest that METTL3 was essential for TGF β 1-induced EMT.

By comparing TGF β 1 expressions between control and Mettl3^{Mut/-} cells, Western blot results surprisingly showed that the expression of TGF β 1 increased in Mettl3^{Mut/-} cells (Figure 1d). Furthermore, up-regulation of TGF β 1 upon extracellular TGF β 1 stimulation was observed in control HeLa cells, which is in line with previous reports (Figure 1d) [32]. However, up-regulation of TGF β 1 was no longer observed in Mettl3^{Mut/-} cells after TGF β 1 stimulation, indicating that METTL3 was involved in the expression of TGF β 1.

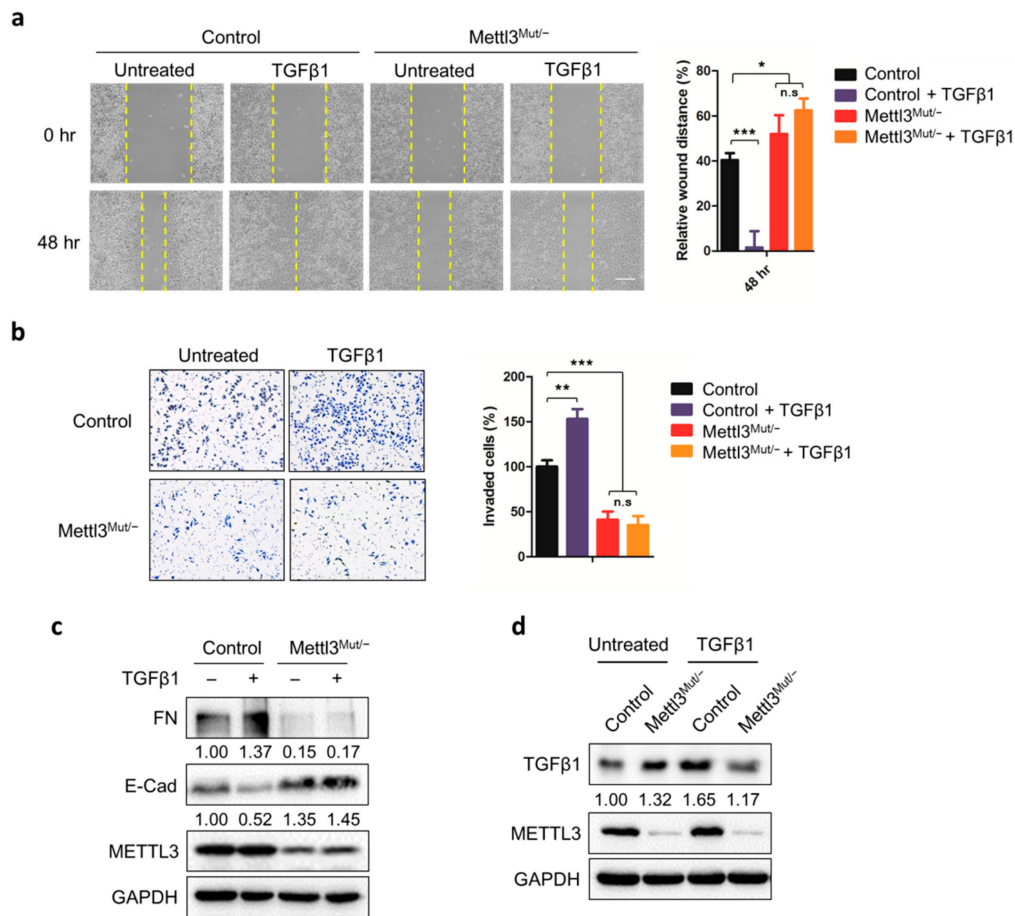


Figure 1. METTL3 regulates EMT and TGFβ1 expression in HeLa cells. **(a)** Control and Mettl3^{Mut/-} HeLa cells were incubated with 10 ng/mL TGFβ1 for indicated times. The wound healing of cells was recorded (left) and quantitatively analyzed (right); scale bar, 100 μm; **(b)** Control and Mettl3^{Mut/-} HeLa cells were incubated with 10 ng/mL TGFβ1 and cells were allowed to invade for 24 h. Invaded cells were tested by CytoSelect™ 24-well Cell Invasion assay kits (8 μm, colorimetric format; left) and quantitatively analyzed (right); **(c)** Control and Mettl3^{Mut/-} HeLa cells were incubated with 10 ng/mL TGFβ1 for 48 h. Protein levels of fibronectin (FN) and E-cadherin (E-Cad) were measured by Western blot. The band intensities of FN and E-Cad were analyzed by ImageJ and listed at the bottom of target bands; **(d)** Control and Mettl3^{Mut/-} HeLa cells were incubated with 10 ng/mL TGFβ1 for 48 h. The protein levels of TGFβ1 in control and Mettl3^{Mut/-} HeLa cells were measured by Western blot. Band intensities of TGFβ1 were analyzed by ImageJ and listed at the bottom of TGFβ1 bands. Data are presented as means ± SD from three independent experiments. Student's *t*-test, n.s, no significant; *, *p* < 0.05; **, *p* < 0.01; ***, *p* < 0.001 compared with control. +, with treatment; −, without treatment.

3.2. m⁶A Negatively Regulates the mRNA Stability of TGFβ1

Considering that METTL3 is critical to mRNA m⁶A methylation, we questioned whether the m⁶A of TGFβ1 mRNA regulated its expression. Firstly, we assumed from the m⁶A sequencing results from our previous study (Accession code GSE112795) [21] that TGFβ1 mRNA contained two m⁶A modification peaks in 5'UTR and exon 1, respectively (Figure 2a). We performed m⁶A RNA-immunoprecipitation (RIP) qPCR and confirmed that m⁶A levels of TGFβ1 mRNA reduced significantly in Mettl3^{Mut/-} cells (Figure 2b). Similarly, the m⁶A levels of TGFβ1 precursor (pre-) mRNA decreased in Mettl3^{Mut/-} cells (Figure 2c). Our data suggested that METTL3 was responsible for the m⁶A modifications on both TGFβ1 mature mRNA and pre-mRNA. By examining the expression of TGFβ1 mRNA, qRT-PCR results showed that mature TGFβ1 levels enhanced significantly (Figure 2d), indicating that m⁶A methylation regulated TGFβ1 expression.

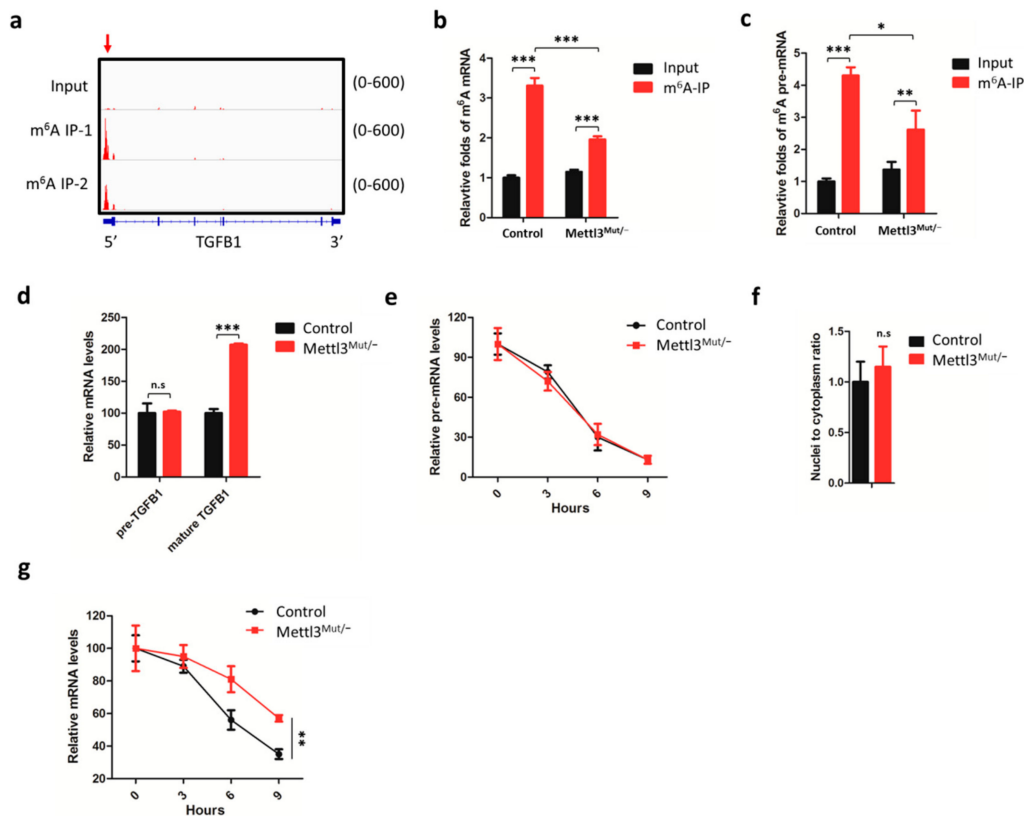


Figure 2. m⁶A triggers TGFB1 mRNA decay in HeLa cells. (a) m⁶A peaks were enriched in the 5'UTR and CDS regions of TGFB1 mRNA from m⁶A RIP-seq data. Arrows marked the m⁶A peaks in HeLa cells. The m⁶A abundance of TGFB1 mRNA is listed on the right; (b) m⁶A RIP-qPCR analysis of TGFB1 mature mRNA in control and Mettl3^{Mut/-} HeLa cells. Input samples were total RNA extracted from control and Mettl3^{Mut/-} HeLa cells. Relative folds of TGFB1 mRNA in m⁶A RIP samples were normalized to the input of control cells; (c) m⁶A RIP-qPCR analysis of TGFB1 precursor (pre-) mRNA in control and Mettl3^{Mut/-} HeLa cells. Relative folds of TGFB1 pre-mRNA in m⁶A RIP samples were normalized to the input of control cells; (d) expression levels of precursor (pre-) and mature mRNA of TGFB1 in control and Mettl3^{Mut/-} HeLa cells were measured by qRT-PCR; (e) Control and Mettl3^{Mut/-} HeLa cells were incubated with 5 μg/mL Act-D for indicated times. Expression levels of TGFB1 pre-mRNA were measured by qRT-PCR; (f) TGFB1 mRNA levels in nuclear and cytoplasmic fractions from control and Mettl3^{Mut/-} HeLa cells were measured by qRT-PCR. Localization of TGFB1 mRNA was calculated as nuclear abundance divided to cytoplasmic abundance; (g) Control and Mettl3^{Mut/-} HeLa cells were incubated with 5 μg/mL Act-D for indicated times. Expression levels of TGFB1 mRNA were measured by qRT-PCR. Data are presented as means ± SD from three independent experiments. Student's *t*-test, n.s., no significant; *, *p* < 0.05; **, *p* < 0.01; ***, *p* < 0.001 compared with control.

Furthermore, we observed that there was no significant differences in pre-mRNA between control and Mettl3^{Mut/-} cells (Figure 2d), suggesting that the pre-mRNA levels of TGFB1 were not affected by m⁶A methylation. Next, we compared the clearance and splicing rate of precursor mRNA (Figure 2e), nuclei-cytoplasm transport (Figure 2f), and stability of TGFB1 mRNA (Figure 2g) between control and Mettl3^{Mut/-} cells. Results showed that the knockdown of METTL3 had no effect on the clearance and splicing rate of precursor mRNA or nuclei-cytoplasm transport of TGFB1 mRNA (Figure 2e,f; Additional file 1: Figure S2). However, the half-life of TGFB1 mature mRNA was longer in Mettl3^{Mut/-} cells compared to control cells, suggesting that m⁶A methylation negatively regulated TGFB1 mRNA decay (Figure 2g).

3.3. m⁶A Negatively Regulates the Translation Elongation of TGFB1 mRNA

We further investigated whether METTL3 may regulate the translation progression of TGFβ1. The effect of METTL3 on the translation process of TGFB1 mRNA was investigated by separating RNA fractions via polysome profiling from control and Mettl3^{Mut/-} cells (Figure 3a). RNA fractionation results suggest that m⁶A modification did not affect the translation initiation process (40S, 60S, and 80S) of TGFB1 mRNA (Figure 3b), but severally enhanced the elongation process (polysome fractions, Figure 3c) in Mettl3^{Mut/-} cells. It indicated that m⁶A may negatively regulate the translation elongation of TGFB1 mRNA.

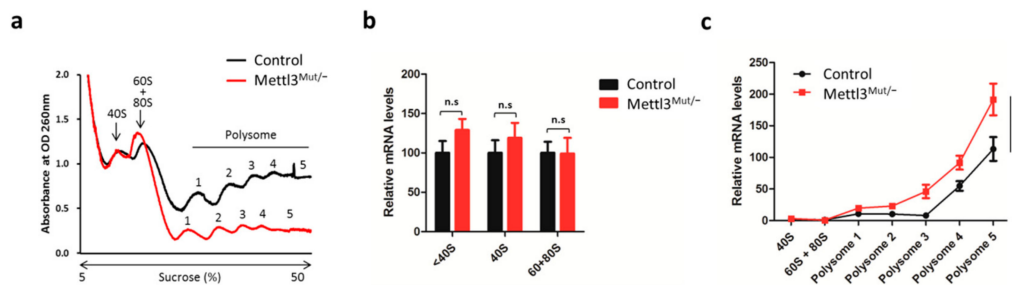


Figure 3. m⁶A modulates translation elongation of TGFB1 mRNA in HeLa cells. (a) Polysome profiles of control and Mettl3^{Mut/-} HeLa cells. Numbers in polysome fraction represent the samples that were used for qRT-PCR in Figure 3c; (b) Expression levels of TGFB1 mRNA in ribosome-unbound (<40S), 40S, and 60 + 80S fractions from control and Mettl3^{Mut/-} HeLa cells; (c) Expression levels of TGFB1 mRNA in 40S, 60 + 80S and polysome fractions from control and Mettl3^{Mut/-} HeLa cells. Data are presented as means ± SD from three independent experiments. Student's *t*-test, n.s, no significant; *, *p* < 0.05 compared with control.

3.4. m⁶A in 5'UTR and CDS Mediates METTL3-Suppressed Translation of TGFB1

We further investigated the potential methylation sites responsible for m⁶A regulated expression of TGFβ1. Firstly, m⁶A-seq data revealed that there was significant enrichment of m⁶A in its CDS and 5'UTR regions (Figure 2a). Thus, two reporters that contained the TGFB1 5'UTR and CDS regions were generated: 1) the 5'UTR region was constructed into the pGL3-basic vector before F-Luc gene, while 2) the CDS region was constructed into the mammalian expression vector. Combining the gene information (Additional file 1: Figure S3a) and m⁶A distribution (Figure 2a) of TGFB1 mRNA, two potential m⁶A sites were targeted: -128A in 5'UTR and 87A in CDS were mutated for study (Figure 4a). To minimize different transfection efficiencies of reporters between control and Mettl3^{Mut/-} cells, transfection amounts of reporters were adjusted. Besides this, mRNA levels of wild-type and mutated reporters were detected in HeLa cells, but no significant difference was observed in both 5'UTR and CDS reporters (Figure 4b).

Firstly, dual-luciferase assay showed that the luciferase production of wild-type 5'UTR reporter was increased in Mettl3^{Mut/-} cells (Figure 4c). Consistently, 5'UTR reporters containing m⁶A mutation also showed increased relative F-Luc values compared to that of wild type reporters (Figure 4d), while there was no significant difference between wild type and mutant reporters in Mettl3^{Mut/-} cells (Additional file 1: Figure S3b). Secondly, Western blot analysis confirmed that the TGFB1 wild-type CDS was increased in Mettl3^{Mut/-} cells (Figure 4e) and the m⁶A mutation can increase the expression of TGFB1 (Figure 4f, Additional file 1: Figure S3c). We further analyzed the translation efficiency by calculating the quotient of reporter protein production divided by mRNA abundance [11]. The results showed that mutations in both 5'UTR and CDS could enhance the translation efficiency of targets (Figure 4g). All these data suggest that m⁶A on TGFB1 mRNA 5'UTR and CDS can suppress its translation, while it has no effect on its mRNA expression.

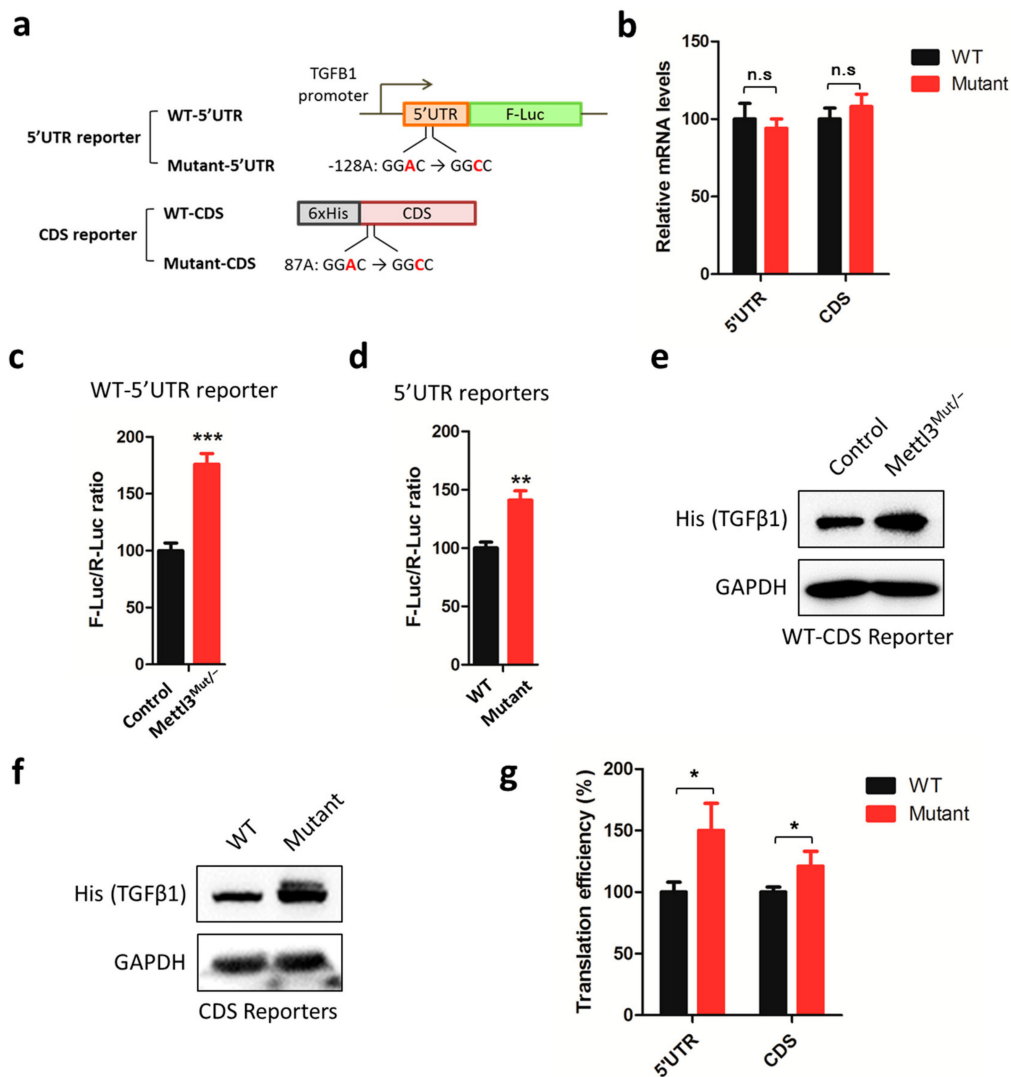


Figure 4. m⁶A methylation on both the 5'UTR and CDS regions of TGFβ1 mRNA controls its translation efficiency. (a) Reporters for 5'UTR and CDS regions of TGFβ1 mRNA. Potential m⁶A sites were mutated (GGAC to GGCC); (b) wild type (WT) and mutated reporters were transfected in HeLa cells for 48 h. Expression levels of reporter mRNA were measured by qRT-PCR: FLUC mRNA for 5'UTR reporter, normalized to RLUC mRNA levels; TGFβ1 mRNA for the CDS reporter, normalized to GAPDH mRNA levels; (c) the WT-5'UTR reporter was co-transfected with TK-Rluc reporter in control and Mettl3^{Mut/-} HeLa cells for 48 h. Dual-luciferase assay was performed to measure F-Luc production, which was normalized to R-Luc levels; (d) WT-5'UTR or Mutant-5'UTR reporter were co-transfected with TK-Rluc reporter in HeLa cells for 48 h. Dual-luciferase assay was performed to measure F-Luc production, which was normalized to R-Luc levels; (e) WT-CDS reporter was transfected in control and Mettl3^{Mut/-} HeLa cells for 48 h. Expression levels of exogenous TGFβ1 (His) were measured by Western blot; (f) WT-CDS or Mutant-CDS reporter were transfected in HeLa cells for 48 h. Expression levels of exogenous TGFβ1 (His) were measured by Western blot; (g) Translation efficiency of WT and TGFβ1 mutant is defined as the quotient of reporter protein production divided by mRNA abundance [11]. For 5'UTR, reporter protein production was determined from dual-luciferase assay; for CDS, reporter protein production was analyzed by ImageJ from Western blot. Data are presented as means ± SD from three independent experiments. Student's *t*-test, n.s, no significant; *, *p* < 0.05; **, *p* < 0.01; ***, *p* < 0.001 compared with control.

3.5. Protein Stability, Secretion, and Activation of TGF β 1 Decreased in *Mettl3*^{Mut/-} Cells

Next, we examined the protein stability of TGF β 1 by incubating cells with protein synthesis inhibitor cycloheximide (CHX). The Western blot results indicate that either the TGF β 1 monomer (mature TGF β 1) or dimer showed a shorter protein half-life in *Mettl3*^{Mut/-} cells (Figure 5a). Similar results were observed in cells treated with TGF β 1 (Additional file 1: Figure S4a). Notably, we observed a $78.4 \pm 3.2\%$ reduction of TGF β 1 dimer formation in *Mettl3*^{Mut/-} cells, compared to TGF β 1 monomer protein amount (Figure 5a), hinting that the secretion of TGF β 1 might be regulated by METTL3. To verify our hypothesis, we detected extracellular TGF β 1 levels by ELISA kit. The results showed that there was $86.5 \pm 3.5\%$ less TGF β 1 secretion in *Mettl3*^{Mut/-} cells compared to control (Figure 5b). After treatment of TGF β 1, the inducing effect of TGF β 1 secretion was no longer observed in *Mettl3*^{Mut/-} cells; rather, it showed a $62.3 \pm 5.8\%$ drop compared to untreated *Mettl3*^{Mut/-} cells.

Considering that the TGF β 1 dimer formation and secretion are regulated by latent TGF β binding proteins (LTBPs), we then compared the expression levels of LTBP1, LTBP2, and LTBP3 between control and *Mettl3*^{Mut/-} cells. qRT-PCR and Western blot results consistently showed that all tested LTBPs decreased significantly in *Mettl3*^{Mut/-} cells (Figure 5c,d). Furthermore, TGF β 1-induced up-regulation of LTBP levels in control cells was no longer observed in *Mettl3*^{Mut/-} cells (Figure 5c,d), suggesting that METTL3 regulated the expression of LTBPs. To confirm this suggestion, we transiently overexpressed LTBP1, which is the most well studied LTBP, in control and *Mettl3*^{Mut/-} cells (Additional file 1: Figure S4b). Western blot results (Figure 5e) showed that the TGF β 1 expression patterns were similar to the untransfected cells shown in Figure 1d. Upon TGF β 1 stimulation, LTBP1 up-regulated TGF β 1 levels in *Mettl3*^{Mut/-} cells as well as control, suggesting that the expression of TGF β 1 was recovered (Figure 5e).

Since the secretion of TGF β 1 is necessary to the activation of TGF β 1/Smad pathway, we detected phosphorylation of SMAD2 (pSMAD2) in both control and *Mettl3*^{Mut/-} cells to investigate whether TGF β 1 activation was regulated by METTL3. Interestingly, both total SMAD2 levels and the pSMAD2 to SMAD2 ratio decreased in *Mettl3*^{Mut/-} cells (Figure 5d). Upon TGF β 1 treatments, pSMAD2 to SMAD2 ratio in *Mettl3*^{Mut/-} cells failed to increase as those in control cells (Figure 5d), suggesting that the activation of TGF β 1 was inhibited in cells lacking METTL3. After re-introducing LTBP1, the pSMAD2 to SMAD2 ratio in *Mettl3*^{Mut/-} cells partially increased from $84.57 \pm 10.02\%$ to $169.91 \pm 23.11\%$ upon TGF β 1 treatments (Figure 5e), suggesting that LTBP1 was not the unique factor affecting TGF β 1 activation. Taken together, our results indicate that protein half-life, secretion, and activation of TGF β 1 were suppressed in *Mettl3*^{Mut/-} cells.

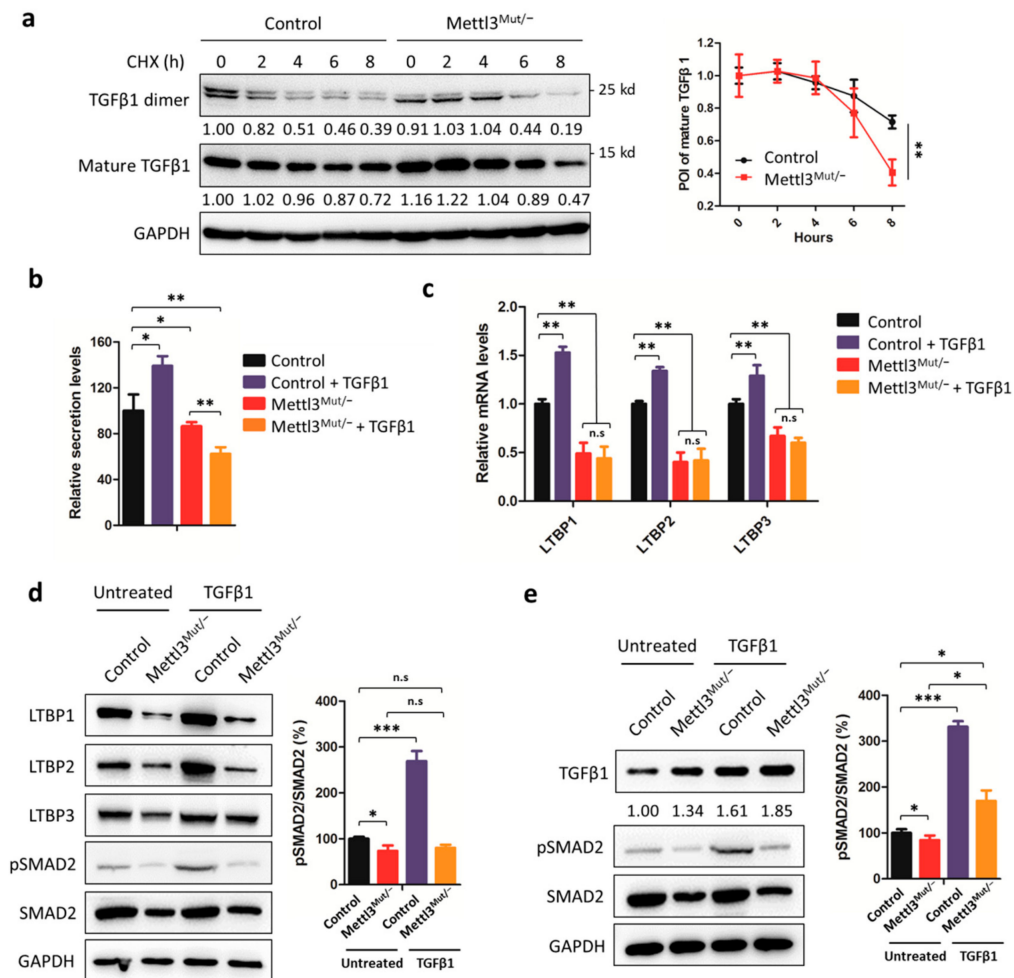


Figure 5. Secretion of TGFβ1 is modulated by METTL3. (a) Control and Mettl3^{Mut/-} HeLa cells were incubated with 100 μg/mL cycloheximide (CHX) for indicated times. Protein levels of mature TGFβ1 and TGFβ1 dimer were measured by Western blot (left). Band intensities were analyzed by ImageJ and are listed at the bottom of target bands. Mature TGFβ1 levels were quantitatively analyzed (right); (b) Control and Mettl3^{Mut/-} HeLa cells were incubated with 10 ng/mL TGFβ1 for 48 h. Secretion of TGFβ1 in control and Mettl3^{Mut/-} HeLa cells was measured by ELISA kit. The relative secretion levels of TGFβ1 were normalized to culture medium with or without the addition of TGFβ1; (c) Control and Mettl3^{Mut/-} HeLa cells were incubated with 10 ng/mL TGFβ1 for 48 h. The expression levels of LTBP1, LTBP2, and LTBP3 mRNA in control and Mettl3^{Mut/-} HeLa cells were measured by qRT-PCR; (d) Control and Mettl3^{Mut/-} HeLa cells were incubated with 10 ng/mL TGFβ1 for 48 h. The expression levels of LTBP1, LTBP2, LTBP3, pSMAD2, and SMAD2 in control and Mettl3^{Mut/-} HeLa cells were measured by Western blot (left). Percentages of pSMAD2 to SMAD2 were analyzed (right); (e) Control and Mettl3^{Mut/-} HeLa cells were transiently overexpressed in LTBP1 for 24 h, then incubated with 10 ng/mL TGFβ1 for 48 h. The expression levels of TGFβ1, pSMAD2, and SMAD2 were measured by Western blot (left). Band intensities of TGFβ1 were analyzed by ImageJ and are listed at the bottom of targets. Percentages of pSMAD2 to SMAD2 were analyzed (right). Data are presented as means ± SD from three independent experiments. Student’s *t*-test, n.s, no significant; *, *p* < 0.05; **, *p* < 0.01; ***, *p* < 0.001 compared with control.

3.6. Snail Is the Key Factor Responsible for TGFβ1-Induced EMT in Mettl3^{Mut/-} Cells

Furthermore, we questioned why TGFβ1 did not stimulate EMT in Mettl3^{Mut/-} cells. Since the TGFβ1-stimulated EMT process can be mediated by Smad signaling, which activates the transcription of EMT transcription factor (EMT-TF) Snail, we verified the expressions of Snail in both control and Mettl3^{Mut/-} cells. As expected, Snail protein levels increased in control cells treated with TGFβ1

(Figure 6a). However, a significant down-regulation of Snail protein was observed in *Mettl3*^{Mut/-} cells, and TGFβ1 stimulation could only increase the limited amount of Snail proteins (Figure 6a). Consistently, the expression of two EMT markers, CDH1 and VIM, which were direct downstream genes of Snail [33], was abolished in TGFβ1-treated *Mettl3*^{Mut/-} cells (Figure 6b). Our results suggest that the inhibition of TGFβ1-induced EMT in *Mettl3*^{Mut/-} cells may due to the down-regulation of Snail.

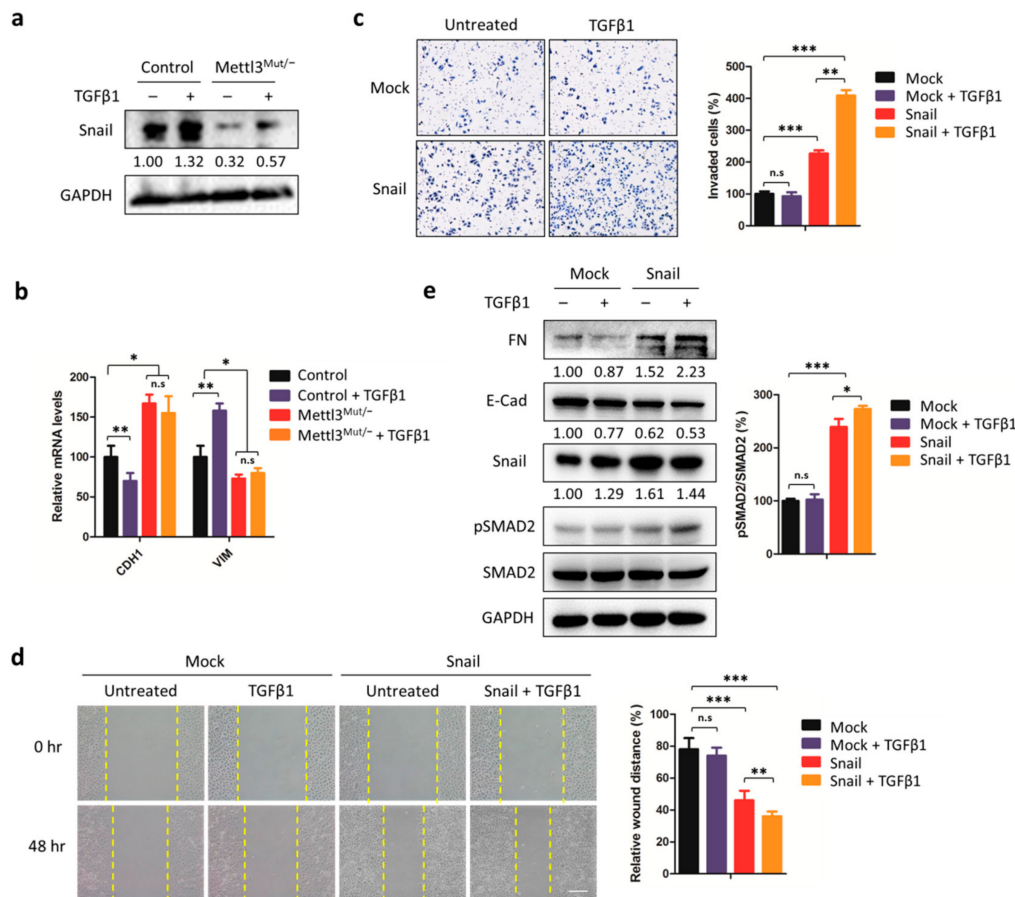


Figure 6. Snail is the core protein responsible for METTL3-mediated EMT. (a) Control and *Mettl3*^{Mut/-} HeLa cells were incubated with 10 ng/mL TGFβ1 for 48 h. The expression levels of Snail were measured by Western blot. Band intensities of Snail were analyzed by ImageJ and are listed at the bottom of target bands; (b) Control and *Mettl3*^{Mut/-} HeLa cells were incubated with 10 ng/mL TGFβ1 for 48 h. Expression levels of CDH1 and VIM mRNA were measured by qRT-PCR; (c) *Mettl3*^{Mut/-} cells transiently overexpressing empty vector (Mock) and Snail were incubated with 10 ng/mL TGFβ1. Cells were allowed to invade for 24 h and were tested by CytoSelect™ 24-well Cell Invasion assay kits (8 μm, colorimetric format; left). Invaded cells were then quantitatively analyzed (right); (d) *Mettl3*^{Mut/-} cells transiently overexpressing empty vector (Mock) and Snail were incubated with 10 ng/mL TGFβ1 for indicated times, and the wound healing of cells was recorded; scale bar, 100 μm; (e) *Mettl3*^{Mut/-} cells transiently overexpressing empty vector (Mock) and Snail were incubated with 10 ng/mL TGFβ1 for 48 h. Expression levels of FN, E-Cad, Snail, pSMAD2, and SMAD2 were measured by Western blot (left). Band intensities of FN, E-Cad, and Snail were analyzed by ImageJ and listed at the bottom of targets. Percentages of pSMAD2 to SMAD2 were analyzed (right). Data are presented as means ± SD from three independent experiments. Student’s *t*-test, n.s., no significant; *, *p* < 0.05; **, *p* < 0.01; ***, *p* < 0.001 compared with control.

In order to reverse the effect of Snail down-regulation in *Mettl3*^{Mut/-} cells, we transiently overexpressed Snail and further examined its effect on cell invasion and migration in vitro. Transwell assay showed that *Mettl3*^{Mut/-} cells overexpressing Snail showed stronger cell invasion ability

(Figure 6c). After TGF β 1 stimulation, cell invasion was significantly enhanced in Mettl3^{Mut/-} cells overexpressing Snail, but not in Mettl3^{Mut/-} cells transfected with empty vector (Mock). Similar results were obtained in wound-healing assays, showing that Mettl3^{Mut/-} cells overexpressing Snail regained the cell migration ability and TGF β 1 treatment further stimulated the migration effect (Figure 6d). Western blot analysis consistently indicated that the overexpression of Snail in Mettl3^{Mut/-} cells induced an increase of FN and decrease of E-cad, and the trends of both FN and E-cad in TGF β 1-treated cells were more obvious than non-treated cells (Figure 6e). By detecting the SMAD2 phosphorylation, results showed that the overexpression of Snail recruited pSMAD2 levels, and TGF β 1 treatments further enhanced the pSMAD2 to SMAD2 ratio (Figure 6e), indicating the TGF β 1 signaling was activated after re-introducing Snail. Together, our results suggest that TGF β 1 can successfully induce the EMT process in Mettl3^{Mut/-} cells overexpressing Snail via Smad signaling.

3.7. METTL3/TGF β 1/Snail Axis Regulates the In Vivo Progression of Cancer

We further tested the potential effects of the METTL3/TGF β 1/Snail axis on the in vivo progression of cancer. We established high lung metastasis potential cancer cell models in our previous studies [21,34] and named them MDA-MB-231^{LMF3} or BT-549^{LMF3} cells. Both qRT-PCR and Western blot analysis showed that the expression of TGF β 1 and METTL3 increased in high lung metastasis potential cancer cells compared with that in the parental cells (Figure 7a,b). To confirm these observations, we used a mammary tumor virus (MMTV) promoter-driven polyoma middle T antigen (PyMT) mice model, which tends to develop secondary metastatic tumors in lungs in tumor-bearing mice [35]. qRT-PCR showed enhanced expression of METTL3 and TGF β 1 in metastasized lung tumors compared to that in the primary tumors isolated from MMTV-PyMT mice (Figure 7c), confirming that METTL3/TGF β 1 triggers cancer progression and metastasis.

We then questioned the possibility of a link between the METTL3/TGF β 1/Snail axis and the clinical development of cervical cancer. TGF β 1 expression in cervical cancer tissues was significantly ($p < 0.01$) greater than that in normal tissues, according to TCGA Cervix (Figure 7d) and Scotto Cervix (Figure 7e) data from the Oncomine database. Furthermore, the mRNA expression of TGF β 1 was negatively correlated with the expression of METTL3 (Figure 7f), while positively correlated with the expression of SNAI1 (Figure 7g) in 169 cases of cervical cancer patients. Using the online bioinformatics tool Kaplan–Meier plotter [36], we found that cervical cancer patients with increased expression of TGF β 1 showed reduced overall survival (OS, Figure 7h). Together, these data suggested that METTL3/TGF β 1/Snail axis regulates the in vivo progression of cancer.

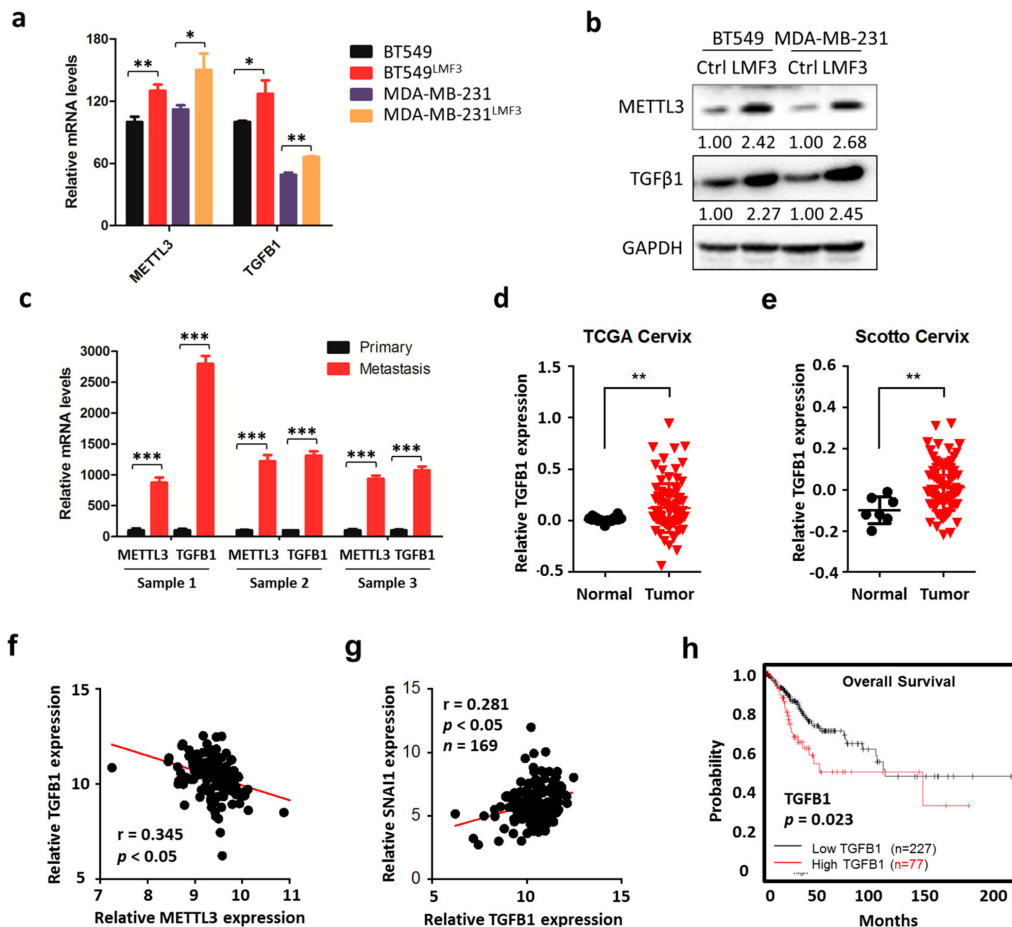


Figure 7. METTL3/TGF β 1/Snail axis regulates the in vivo progression of cancer. (a) Expression levels of METTL3 and TGF β 1 mRNA in MDA-MB-231^{LMF3} or BT-549^{LMF3} cells and their corresponding parental cells were measured by qRT-PCR; (b) expression levels of METTL3 and TGF β 1 in MDA-MB-231^{LMF3} or BT-549^{LMF3} cells (LMF3) and their corresponding parental cells (Ctrl) were measured by Western blot. Band intensities of METTL3 and TGF β 1 were analyzed by ImageJ and are listed at the bottom of target bands; (c) expression levels of METTL3 and TGF β 1 mRNA in primary tumors and metastasized tumors in lungs isolated from three MMTV-PyMT mice were measured by qRT-PCR. Data are presented as means \pm SD from three technical replicates. (d) Expression of TGF β 1 in cervical tumor tissues and normal tissues from Oncomine database: Ma Breast 4; (e) Expression of TGF β 1 in cervical tumor tissues and normal tissues from Oncomine database: Cluck Breast; (f) Pearson correlation between TGF β 1 and METTL3 in 169 cervical cancer tissues from the TCGA database; (g) Pearson correlation between TGF β 1 and SNAI1 in 169 cervical cancer tissues from the TCGA database; (h) Overall survival (OS) in patients with high ($n = 227$) versus low ($n = 77$) levels of TGF β 1 in cervical cancer patients plotted by the Kaplan–Meier method. Data in Figure 7a are presented as means \pm SD from three independent experiments. Student’s *t*-test, *, $p < 0.05$; **, $p < 0.01$ compared with control.

4. Discussion

In the present study, we showed that TGF β 1 failed to induce EMT in *Mettl3*^{Mut/−} cells, and the TGF β 1-induced up-regulation of TGF β 1 was inhibited. On one hand, we found that the expression of TGF β 1 was modulated by m⁶A, and that m⁶A methylation on TGF β 1 mRNA enhanced its mRNA decay and reduced translation. Besides this, the dimer formation of TGF β 1, which is necessary for its autocrine, was suppressed in *Mettl3*^{Mut/−} cells. On the other hand, we demonstrated that a lack of METTL3 suppressed activation of TGF β 1, and the down-regulation of Snail in *Mettl3*^{Mut/−} cells was responsible for the failure of the TGF β 1-induced EMT process.

Increasing evidence suggests that METTL3 is involved in the progression of cancer cells [18,37,38]. Consistent with previous report [21], we revealed that TGF β 1 failed to induce EMT in the absence of METTL3, indicating the critical role of METTL3 in the EMT process of HeLa cells. Furthermore, SMAD2 and Snail, effectors of TGF β 1 signaling and EMT-inducing transcription factor, respectively, were down-regulated in *Mettl3*^{Mut/-} cells, indicating that the abolishment of TGF β 1 signaling and suppressed translation of Snail [21] are related to this EMT inhibition. TGF β signaling plays a prominent role in EMT development, among a plethora of signaling pathways [22]. Here, we reported that METTL3 modulated TGF β 1 signaling both extracellularly and intracellularly. On one hand, down-regulation of LTBP decreased free TGF β 1 binding to receptors, which therefore suppressed the TGF β 1 signaling initiation [39]. On the other hand, both SMAD2 and pSMAD2 were down-regulated in *Mettl3*^{Mut/-} cells, suggesting the TGF β /Smad signal was inhibited. Despite our observations, a novel link between SMADs and m⁶A methylation has been reported recently, showing that SMAD2/3 colocalizes with the METTL3–METTL14–WTAP complex and promotes binding of the m⁶A methyltransferase complex onto targets [40]. This shows the possibility that there may be a mutual benefit between TGF β /Smad signal and m⁶A methylation, and co-regulation of biological processes, including EMT.

m⁶A methylation-modulated EMT via Snail expression has been reported [21]. Here, we consistently showed that *Mettl3*^{Mut/-} cells transiently recruiting Snail performed TGF β 1-induced EMT behaviors, suggesting the critical role of Snail in TGF β 1-induced EMT. The TGF β 1-induced transition of EMT is accomplished by Smad signals, which enhances the Snail expression and further activates the transcription of EMT factors, such as down-regulation of E-cad and up-regulation of Vim [33]. Notably, we observed that the overexpression of Snail can enhance pSMAD2 levels, which was inhibited in *Mettl3*^{Mut/-} cells, indicating that there is a positive regulation of Snail on Smad signaling. Furthermore, we showed that there is strong correlation between the METTL3/TGF β 1/Snail axis and cancer progression in lung metastasis potential cancer cell models. By analyzing clinical data of cervical cancer, the correlation between METTL3 and TGF β 1 was relatively weak, which was mainly due to the inclusion of primary cervical cancer cases. Increasing reports show that metastatic dissemination can occur from the earliest point of tumorigenesis, prior to the clinical manifestation of tumors [41–43], indicating that the primary tumors also have metastatic potential. However, the TGF β 1 levels in primary cancer are commonly lower than in metastatic cancer [44], which therefore may affect the correlation analysis. Together, our data demonstrated that both METTL3 and Snail play key roles in responding to TGF β 1 signals in HeLa cells undergoing the EMT process.

Functions of m⁶A on mRNA translation have been studied for years. However, the exact role of m⁶A on the translation process is unknown. Wang et al. [11] revealed that 3'UTR m⁶A recruited reader protein YTHDF1 and promoted the circulation of mRNA to improve translation efficiency. Zhou et al. [45] demonstrated that 5'UTR m⁶A regulated the reinitiation and controlling alternative translation of ATF4 mRNA. Later, Lin et al. [21] revealed that CDS m⁶A triggered SNAI translation via YTHDF1 and eEF-2 interaction. It seems that localization of m⁶A may be critical to the translation regulation of their targets. Here, we reported that TGF β 1 translation was inhibited when m⁶A modification existed. According to m⁶A-seq results (Figure 2a), two obvious m⁶A modification signals were observed in 5'UTR and at the beginning of the CDS of TGF β 1 mRNA, with 386.3 \pm 88.2% and 115.5 \pm 33.5% abundance, respectively. Interestingly, mutations of potential m⁶A methylation sites in both 5'UTR and CDS can enhance target expressions (Figure 4d,f), which was due to the increase of translation efficiency (Figure 4g). It is possible that m⁶A methylation on TGF β 1 mRNA decreases the elongation efficiency during the translation process (Figure 3c). However, the detailed mechanism of how m⁶A methylation regulation TGF β 1 translation remains to be elucidated.

TGF β 1 can autocrine from cells and further stimulates its own expression through the up-regulation of TGF β receptors, which stimulate TGF β 1 expression and sustain signaling for the long process of EMT [22,27,32]. The activation of TGF β is achieved by the cleavage of TGF β propeptide, called the latency-associated protein (LAP), which is accomplished by LTBP interaction [46,47]. After dissociating TGF β from LAP, TGF β is secreted in a latent form, containing LTBP, TGF β dimer, and non-covalent

binding LAPs. LTBP3s are essential to maintain TGF β latency and target the latent TGF β to extracellular matrix (ECM) [39]. Our data revealed that expressions of LTBP3s were suppressed in *Mettl3*^{Mut/-} cells, even under TGF β 1 stimulation conditions, leading to failure of the TGF β 1 dimer formation, therefore inhibiting the TGF β 1 activation. This hypothesis was further confirmed by the rescue experiment, which shows that the overexpression of LTBP1 can recover the TGF β 1 expression in *Mettl3*^{Mut/-} cells (Figure 5e). Based on our m⁶A-seq results (accession code GSE112795) [21], only LTBP3 contained significant m⁶A modifications on its mRNA (Additional file 1: Figure S5), indicating that METTL3 probably regulated LTBP expression indirectly, despite modulating mRNA behaviors of LTBP3s. Remarkably, TGF β 1 levels can be affected by many other factors, such as growth factors and kinases, generating positive feed-forward loops necessary for sustained signaling that supports the EMT process [22,27].

We revealed that m⁶A methylation was critical to the EMT process of HeLa cells. We demonstrated that m⁶A methylation played at least three distinct roles in TGF β 1-induced EMT regulation—modulating TGF β 1 mRNA decay and translation, TGF β 1 activation, and Snail expression—suggesting the multiple roles of m⁶A in cancer progression regulation. Notably, the regulation of METTL3 on TGF β 1-induced EMT might be cell type-dependent. The contribution of m⁶A in cancer metastasis in other types of cancer cells requires further investigation.

Supplementary Materials: The following are available online at <http://www.mdpi.com/2073-4409/9/2/296/s1>, Figure S1: METTL3 regulates EMT in HeLa cells. (a) m⁶A/A ratio of total mRNA from control and *Mettl3*^{Mut/-} cells were determined by LC-MS/MS; (b) *Mettl3*^{Mut/-} cells transiently overexpressed METTL3 and then incubated with 10 ng/mL TGF β 1 for indicated times. The wound healing of cells was recorded (left) and quantitatively analyzed (right); scale bar, 100 μ m; (c) *Mettl3*^{Mut/-} cells transiently overexpressed METTL3 and then incubated with 10 ng/mL TGF β 1 and cells were allowed to invade for 24 h. Invaded cells were tested by CytoSelect™ 24-well Cell Invasion assay kits (8 μ m, colorimetric format; left) and quantitatively analyzed (right); (d) *Mettl3*^{Mut/-} cells transiently overexpressed METTL3 and then incubated with or without 10 ng/mL TGF β 1 for 48 h. Protein levels of FN, E-Cad and METTL3 were measured by Western blot. Figure S2: Quality control for fractionation. Cytoplasmic (C) and nuclear (N) fractions were separated from control and *Mettl3*^{Mut/-} cells, respectively. Cytoplasmic marker GAPDH and nuclear marker H2A-X were detected by Western blot. Figure S3: m⁶A methylation on both 5'UTR and CDS regions of TGF β 1 mRNA control its translation efficiency. (a) Sequence of TGF β 1 mRNA 5'UTR and CDS region (XM_011527242.2). TGF β 1 5'UTR region is marked in blue. Mutation sites of potential m⁶A motifs were highlighted in red (mutation site: GGAC to GGCC); (b) WT-5'UTR or Mutant-5'UTR reporter was co-transfected with TK-Rluc reporter in *Mettl3*^{Mut/-} cells for 48 h. Dual-luciferase assay was performed to measure F-Luc production, which was normalized to R-Luc levels; (c) WT-CDS or Mutant-CDS reporter was transfected in control or *Mettl3*^{Mut/-} cells as indicated for 48 h. Expression levels of exogenous TGF β 1 (His) were measured by Western blot. Figure S4: Protein stability and secretion of TGF β 1 are modulated by METTL3. (a) Control and *Mettl3*^{Mut/-} cells were incubated with 10 ng/mL TGF β 1 for 48 h. 100 μ g/mL cycloheximide (CHX) was added into cells for indicated times. Protein levels of mature TGF β 1 and TGF β 1 dimer were measured by Western blot (left). Band intensities were analyzed by ImageJ and listed at the bottom of target bands. Mature TGF β 1 levels were quantitatively analyzed (right); (b) Empty vector (Mock) and HA-LTBP1 vector were transiently overexpressed in Control and *Mettl3*^{Mut/-} cells. Expression levels of exogenous LTBP1 were detected by Western blot. Figure S5: m⁶A peaks of LTBP1, LTBP2, LTBP3 in HeLa cells. m⁶A peak distributions of LTBP1, LTBP2 and LTBP3 mRNA from m⁶A RIP-seq data (Accession code GSE112795). m⁶A abundance of mRNA was listed on the right. Table S1: Primers for mutagenesis.

Author Contributions: J.L., conceptualization, writing—original draft preparation, investigation, funding acquisition; F.C., methodology and software; Y.P., validation and data curation; Z.L., investigation; X.L., formal analysis; Z.C., supervision; H.W., writing—review and editing, funding acquisition and project administration. All authors have read and agreed to the published version of the manuscript.

Funding: This research was funded by the National Natural Science Foundation of China (Grant Nos. 31801197, 81973343, 81673454, and 81672608) and the China Postdoctoral Science Foundation (Grant No. 2018M643354), the Fundamental Research Funds for the Central Universities (Sun Yat-sen University) (Nos.19ykpy130 and 19ykzd24), the Guangdong Provincial Key Laboratory of Construction Foundation (No. 2017B030314030).

Acknowledgments: The authors thank the study investigators and staff who participated in this study.

Conflicts of Interest: The authors declare no conflict of interest.

References

1. Dubin, D.T.; Taylor, R.H. The methylation state of poly A-containing messenger RNA from cultured hamster cells. *Nucleic Acids Res.* **1975**, *2*, 1653–1668. [[CrossRef](#)] [[PubMed](#)]
2. Roundtree, I.A.; Evans, M.E.; Pan, T.; He, C. Dynamic RNA Modifications in Gene Expression Regulation. *Cell* **2017**, *169*, 1187–1200. [[CrossRef](#)] [[PubMed](#)]
3. Zhang, S. Mechanism of N(6)-methyladenosine modification and its emerging role in cancer. *Pharmacol. Ther.* **2018**, *189*, 173–183. [[CrossRef](#)] [[PubMed](#)]
4. Jia, G.; Fu, Y.; Zhao, X.; Dai, Q.; Zheng, G.; Yang, Y.; Yi, C.; Lindahl, T.; Pan, T.; Yang, Y.G.; et al. N6-methyladenosine in nuclear RNA is a major substrate of the obesity-associated FTO. *Nat. Chem. Biol.* **2011**, *7*, 885–887. [[CrossRef](#)] [[PubMed](#)]
5. Zheng, G.; Dahl, J.A.; Niu, Y.; Fedorcsak, P.; Huang, C.M.; Li, C.J.; Vagbo, C.B.; Shi, Y.; Wang, W.L.; Song, S.H.; et al. ALKBH5 is a mammalian RNA demethylase that impacts RNA metabolism and mouse fertility. *Mol. Cell* **2013**, *49*, 18–29. [[CrossRef](#)] [[PubMed](#)]
6. Bartosovic, M.; Molaes, H.C.; Gregorova, P.; Hrossova, D.; Kudla, G.; Vanacova, S. N6-methyladenosine demethylase FTO targets pre-mRNAs and regulates alternative splicing and 3'-end processing. *Nucleic Acids Res.* **2017**, *45*, 11356–11370. [[CrossRef](#)]
7. Haussmann, I.U.; Bodi, Z.; Sanchez-Moran, E.; Mongan, N.P.; Archer, N.; Fray, R.G.; Soller, M. m(6)A potentiates Sxl alternative pre-mRNA splicing for robust Drosophila sex determination. *Nature* **2016**, *540*, 301–304. [[CrossRef](#)]
8. Lence, T.; Akhtar, J.; Bayer, M.; Schmid, K.; Spindler, L.; Ho, C.H.; Kreim, N.; Andrade-Navarro, M.A.; Poeck, B.; Helm, M.; et al. m(6)A modulates neuronal functions and sex determination in Drosophila. *Nature* **2016**, *540*, 242–247. [[CrossRef](#)]
9. Fustin, J.M.; Doi, M.; Yamaguchi, Y.; Hida, H.; Nishimura, S.; Yoshida, M.; Isagawa, T.; Morioka, M.S.; Kakeya, H.; Manabe, I.; et al. RNA-methylation-dependent RNA processing controls the speed of the circadian clock. *Cell* **2013**, *155*, 793–806. [[CrossRef](#)]
10. Roundtree, I.A.; Luo, G.Z.; Zhang, Z.; Wang, X.; Zhou, T.; Cui, Y.; Sha, J.; Huang, X.; Guerrero, L.; Xie, P.; et al. YTHDC1 mediates nuclear export of N(6)-methyladenosine methylated mRNAs. *eLife* **2017**, *6*, e31311. [[CrossRef](#)]
11. Wang, X.; Zhao, B.S.; Roundtree, I.A.; Lu, Z.; Han, D.; Ma, H.; Weng, X.; Chen, K.; Shi, H.; He, C. N(6)-methyladenosine Modulates Messenger RNA Translation Efficiency. *Cell* **2015**, *161*, 1388–1399. [[CrossRef](#)] [[PubMed](#)]
12. Wang, X.; Lu, Z.; Gomez, A.; Hon, G.C.; Yue, Y.; Han, D.; Fu, Y.; Parisien, M.; Dai, Q.; Jia, G.; et al. N6-methyladenosine-dependent regulation of messenger RNA stability. *Nature* **2014**, *505*, 117–120. [[CrossRef](#)] [[PubMed](#)]
13. Choe, J.; Lin, S.; Zhang, W.; Liu, Q.; Wang, L.; Ramirez-Moya, J.; Du, P.; Kim, W.; Tang, S.; Sliz, P.; et al. mRNA circularization by METTL3-eIF3h enhances translation and promotes oncogenesis. *Nature* **2018**, *561*, 556–560. [[CrossRef](#)] [[PubMed](#)]
14. Lin, S.; Choe, J.; Du, P.; Triboulet, R.; Gregory, R.I. The m(6)A Methyltransferase METTL3 Promotes Translation in Human Cancer Cells. *Mol. Cell* **2016**, *62*, 335–345. [[CrossRef](#)]
15. Sledz, P.; Jinek, M. Structural insights into the molecular mechanism of the m(6)A writer complex. *eLife* **2016**, *5*, e18434. [[CrossRef](#)]
16. Wang, X.; Feng, J.; Xue, Y.; Guan, Z.; Zhang, D.; Liu, Z.; Gong, Z.; Wang, Q.; Huang, J.; Tang, C.; et al. Structural basis of N(6)-adenosine methylation by the METTL3-METTL14 complex. *Nature* **2016**, *534*, 575–578. [[CrossRef](#)]
17. Wang, P.; Doxtader, K.A.; Nam, Y. Structural Basis for Cooperative Function of Mettl3 and Mettl14 Methyltransferases. *Mol. Cell* **2016**, *63*, 306–317. [[CrossRef](#)]
18. Pan, Y.; Ma, P.; Liu, Y.; Li, W.; Shu, Y. Multiple functions of m(6)A RNA methylation in cancer. *J. Hematol. Oncol.* **2018**, *11*, 48. [[CrossRef](#)]
19. Wang, S.; Chai, P.; Jia, R.; Jia, R. Novel insights on m(6)A RNA methylation in tumorigenesis: A double-edged sword. *Mol. Cancer* **2018**, *17*, 101. [[CrossRef](#)]

20. Barbieri, I.; Tzelepis, K.; Pandolfini, L.; Shi, J.; Millan-Zambrano, G.; Robson, S.C.; Aspris, D.; Migliori, V.; Bannister, A.J.; Han, N.; et al. Promoter-bound METTL3 maintains myeloid leukaemia by m(6)A-dependent translation control. *Nature* **2017**, *552*, 126–131. [[CrossRef](#)]
21. Lin, X.; Chai, G.; Wu, Y.; Li, J.; Chen, F.; Liu, J.; Luo, G.; Tauler, J.; Du, J.; Lin, S.; et al. RNA m(6)A methylation regulates the epithelial mesenchymal transition of cancer cells and translation of Snail. *Nat. Commun.* **2019**, *10*, 2065. [[CrossRef](#)] [[PubMed](#)]
22. Tsubakihara, Y.; Moustakas, A. Epithelial-Mesenchymal Transition and Metastasis under the Control of Transforming Growth Factor beta. *Int. J. Mol. Sci.* **2018**, *19*, 3672. [[CrossRef](#)] [[PubMed](#)]
23. Saharinen, J.; Keski-Oja, J. Specific sequence motif of 8-Cys repeats of TGF-beta binding proteins, LTBP, creates a hydrophobic interaction surface for binding of small latent TGF-beta. *Mol. Biol. Cell* **2000**, *11*, 2691–2704. [[CrossRef](#)] [[PubMed](#)]
24. Lack, J.; O’Leary, J.M.; Knott, V.; Yuan, X.; Rifkin, D.B.; Handford, P.A.; Downing, A.K. Solution structure of the third TB domain from LTBP1 provides insight into assembly of the large latent complex that sequesters latent TGF-beta. *J. Mol. Biol.* **2003**, *334*, 281–291. [[CrossRef](#)] [[PubMed](#)]
25. Chandramouli, A.; Simundza, J.; Pinderhughes, A.; Cowin, P. Choreographing metastasis to the tune of LTBP. *J. Mammary Gland Biol. Neoplasia* **2011**, *16*, 67–80. [[CrossRef](#)] [[PubMed](#)]
26. Moustakas, A.; Heldin, C.H. Mechanisms of TGFbeta-Induced Epithelial-Mesenchymal Transition. *J. Clin. Med.* **2016**, *5*, 63. [[CrossRef](#)]
27. Ye, X.; Weinberg, R.A. Epithelial-Mesenchymal Plasticity: A Central Regulator of Cancer Progression. *Trends Cell Biol.* **2015**, *25*, 675–686. [[CrossRef](#)]
28. Yue, Y.; Liu, J.; Cui, X.; Cao, J.; Luo, G.; Zhang, Z.; Cheng, T.; Gao, M.; Shu, X.; Ma, H.; et al. VIRMA mediates preferential m(6)A mRNA methylation in 3’UTR and near stop codon and associates with alternative polyadenylation. *Cell Discov.* **2018**, *4*, 10. [[CrossRef](#)]
29. Li, J.; Lam, W.W.; Lai, T.W.; Au, S.W. Degradation of nuclear Ubc9 induced by listeriolysin O is dependent on K(+) efflux. *Biochem. Biophys. Res. Commun.* **2017**, *493*, 1115–1121. [[CrossRef](#)]
30. Li, Z.; Weng, H.; Su, R.; Weng, X.; Zuo, Z.; Li, C.; Huang, H.; Nachtergaele, S.; Dong, L.; Hu, C.; et al. FTO Plays an Oncogenic Role in Acute Myeloid Leukemia as a N6-Methyladenosine RNA Demethylase. *Cancer Cell* **2017**, *31*, 127–141. [[CrossRef](#)]
31. Liang, X.H.; Sun, H.; Nichols, J.G.; Croke, S.T. RNase H1-Dependent Antisense Oligonucleotides Are Robustly Active in Directing RNA Cleavage in Both the Cytoplasm and the Nucleus. *Mol. Ther. J. Am. Soc. Gene Ther.* **2017**, *25*, 2075–2092. [[CrossRef](#)] [[PubMed](#)]
32. Duan, D.; Derynck, R. Transforming growth factor-beta (TGF-beta)-induced up-regulation of TGF-beta receptors at the cell surface amplifies the TGF-beta response. *J. Biol. Chem.* **2019**, *294*, 8490–8504. [[CrossRef](#)] [[PubMed](#)]
33. Zeisberg, M.; Neilson, E.G. Biomarkers for epithelial-mesenchymal transitions. *J. Clin. Investig.* **2009**, *119*, 1429–1437. [[CrossRef](#)] [[PubMed](#)]
34. Lu, L.; Chen, Z.; Lin, X.; Tian, L.; Su, Q.; An, P.; Li, W.; Wu, Y.; Du, J.; Shan, H.; et al. Inhibition of BRD4 suppresses the malignancy of breast cancer cells via regulation of Snail. *Cell Death Differ.* **2019**. [[CrossRef](#)] [[PubMed](#)]
35. Guy, C.T.; Cardiff, R.D.; Muller, W.J. Induction of mammary tumors by expression of polyomavirus middle T oncogene: A transgenic mouse model for metastatic disease. *Mol. Cell. Biol.* **1992**, *12*, 954–961. [[CrossRef](#)] [[PubMed](#)]
36. Szasz, A.M.; Lanczky, A.; Nagy, A.; Forster, S.; Hark, K.; Green, J.E.; Boussioutas, A.; Busuttill, R.; Szabo, A.; Gyorffy, B. Cross-validation of survival associated biomarkers in gastric cancer using transcriptomic data of 1065 patients. *Oncotarget* **2016**, *7*, 49322–49333. [[CrossRef](#)]
37. Panneerdoss, S.; Eedunuri, V.K.; Yadav, P.; Timilsina, S.; Rajamanickam, S.; Viswanadhappalli, S.; Abdelfattah, N.; Onyeagucha, B.C.; Cui, X.; Lai, Z.; et al. Cross-talk among writers, readers, and erasers of m(6)A regulates cancer growth and progression. *Sci. Adv.* **2018**, *4*, eaar8263. [[CrossRef](#)]
38. Liu, J.; Eckert, M.A.; Harada, B.T.; Liu, S.M.; Lu, Z.; Yu, K.; Tienda, S.M.; Chryplewicz, A.; Zhu, A.C.; Yang, Y.; et al. m(6)A mRNA methylation regulates AKT activity to promote the proliferation and tumorigenicity of endometrial cancer. *Nat. Cell Biol.* **2018**, *20*, 1074–1083. [[CrossRef](#)]
39. Robertson, I.B.; Horiguchi, M.; Zilberberg, L.; Dabovic, B.; Hadjiolova, K.; Rifkin, D.B. Latent TGF-beta-binding proteins. *Matrix Biol. J. Int. Soc. Matrix Biol.* **2015**, *47*, 44–53. [[CrossRef](#)]

40. Bertero, A.; Brown, S.; Madrigal, P.; Osnato, A.; Ortmann, D.; Yiangou, L.; Kadiwala, J.; Hubner, N.C.; de Los Mozos, I.R.; Sadee, C.; et al. The SMAD2/3 interactome reveals that TGFbeta controls m(6)A mRNA methylation in pluripotency. *Nature* **2018**, *555*, 256–259. [[CrossRef](#)]
41. Harper, K.L.; Sosa, M.S.; Entenberg, D.; Hosseini, H.; Cheung, J.F.; Nobre, R.; Avivar-Valderas, A.; Nagi, C.; Girmius, N.; Davis, R.J.; et al. Mechanism of early dissemination and metastasis in Her2(+) mammary cancer. *Nature* **2016**, *540*, 588–592. [[CrossRef](#)]
42. Hosseini, H.; Obradovic, M.M.S.; Hoffmann, M.; Harper, K.L.; Sosa, M.S.; Werner-Klein, M.; Nanduri, L.K.; Werno, C.; Ehrl, C.; Maneck, M.; et al. Early dissemination seeds metastasis in breast cancer. *Nature* **2016**, *540*, 552–558. [[CrossRef](#)] [[PubMed](#)]
43. Klein, C.A. Parallel progression of primary tumours and metastases. *Nat. Rev. Cancer* **2009**, *9*, 302–312. [[CrossRef](#)] [[PubMed](#)]
44. Tan, E.J.; Olsson, A.K.; Moustakas, A. Reprogramming during epithelial to mesenchymal transition under the control of TGFbeta. *Cell Adhes. Migr.* **2015**, *9*, 233–246. [[CrossRef](#)] [[PubMed](#)]
45. Zhou, J.; Wan, J.; Shu, X.E.; Mao, Y.; Liu, X.M.; Yuan, X.; Zhang, X.; Hess, M.E.; Bruning, J.C.; Qian, S.B. N(6)-Methyladenosine Guides mRNA Alternative Translation during Integrated Stress Response. *Mol. Cell* **2018**, *69*, 636–647. [[CrossRef](#)] [[PubMed](#)]
46. Rifkin, D.B. Latent transforming growth factor-beta (TGF-beta) binding proteins: Orchestrators of TGF-beta availability. *J. Biol. Chem.* **2005**, *280*, 7409–7412. [[CrossRef](#)]
47. Robertson, I.B.; Rifkin, D.B. Regulation of the Bioavailability of TGF-beta and TGF-beta-Related Proteins. *Cold Spring Harb. Perspect. Biol.* **2016**, *8*, a021907. [[CrossRef](#)]



© 2020 by the authors. Licensee MDPI, Basel, Switzerland. This article is an open access article distributed under the terms and conditions of the Creative Commons Attribution (CC BY) license (<http://creativecommons.org/licenses/by/4.0/>).